

The GEWEX water vapor assessment (G-VAP)

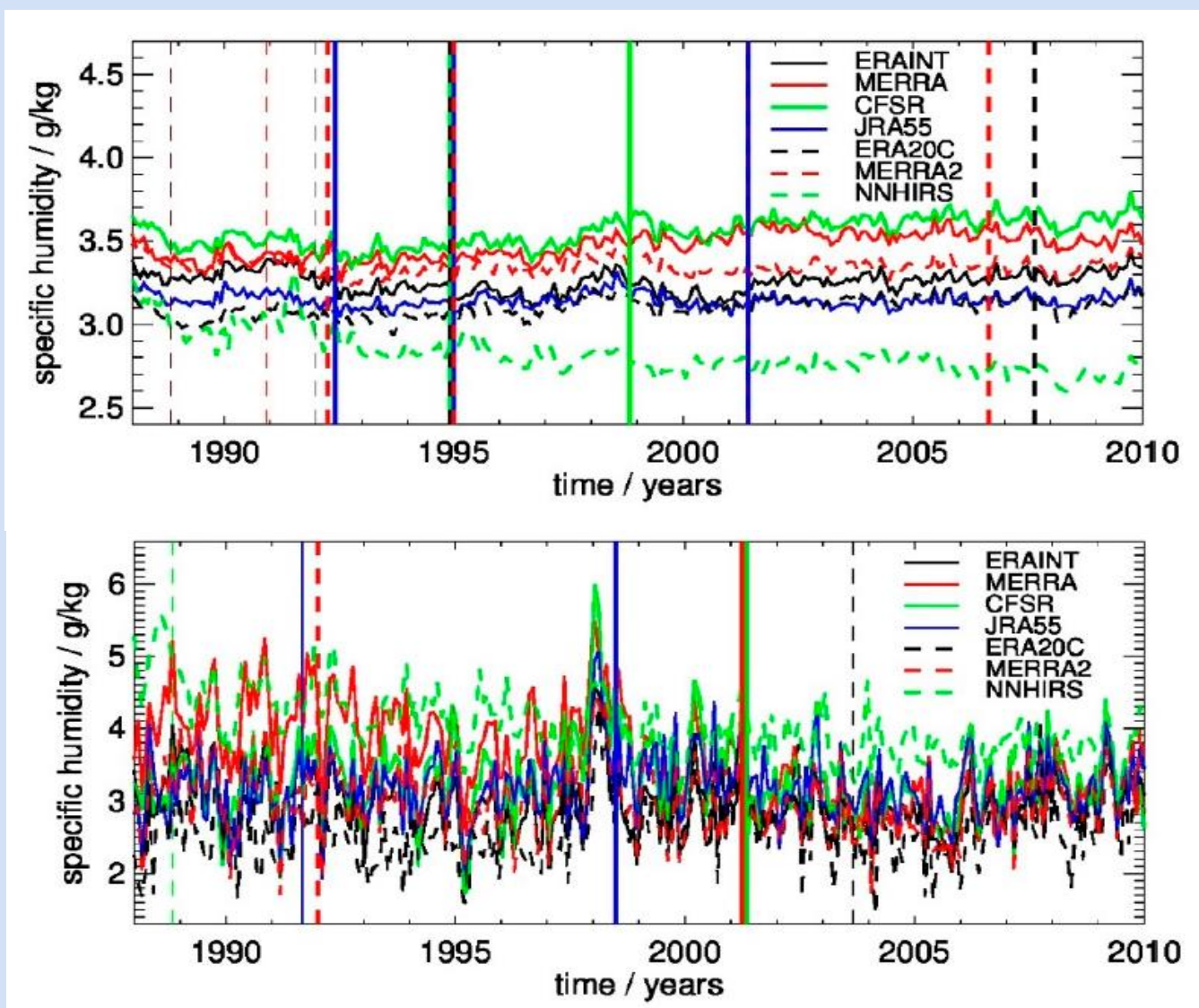
Marc Schröder¹, Helene Brogniez², Shu-peng Ho³ and the G-VAP community

¹Deutscher Wetterdienst, Offenbach, Germany, ²LATMOS, U. Paris-Saclay, Paris, France, ³NOAA, College Park, USA

The GEWEX water vapor assessment (G-VAP) was initiated by the GEWEX Data and Analysis Panel (GDAP). The major purpose of G-VAP is to quantify the state of the art in water vapour products being constructed for climate applications, and by this support the selection process of suitable water vapour products by GDAP (see gewex-vap.org).

The assessment provides an overview of available data records (see gewex-vap.org → Data Records) and results based on consistent product inter-comparisons and comparisons to ground-based and in-situ observations. TCWV (total column water vapour), upper tropospheric humidity and profiles of specific humidity and temperature are considered. A focus is on the assessment of temporal homogeneity and consistently computed trend estimates are also analysed. The inter-comparison results presented here consider eleven of the long-term TCWV and seven water vapour profile data records, namely ERA-20C, ERA-Interim, HOAPS, JRA55, MERRA, MERRA2, NCEP/CFR, nnHIRS, NVAP-M, NVAP-Ocean, REMSS.

Homogeneity and compliance with changes in observing system

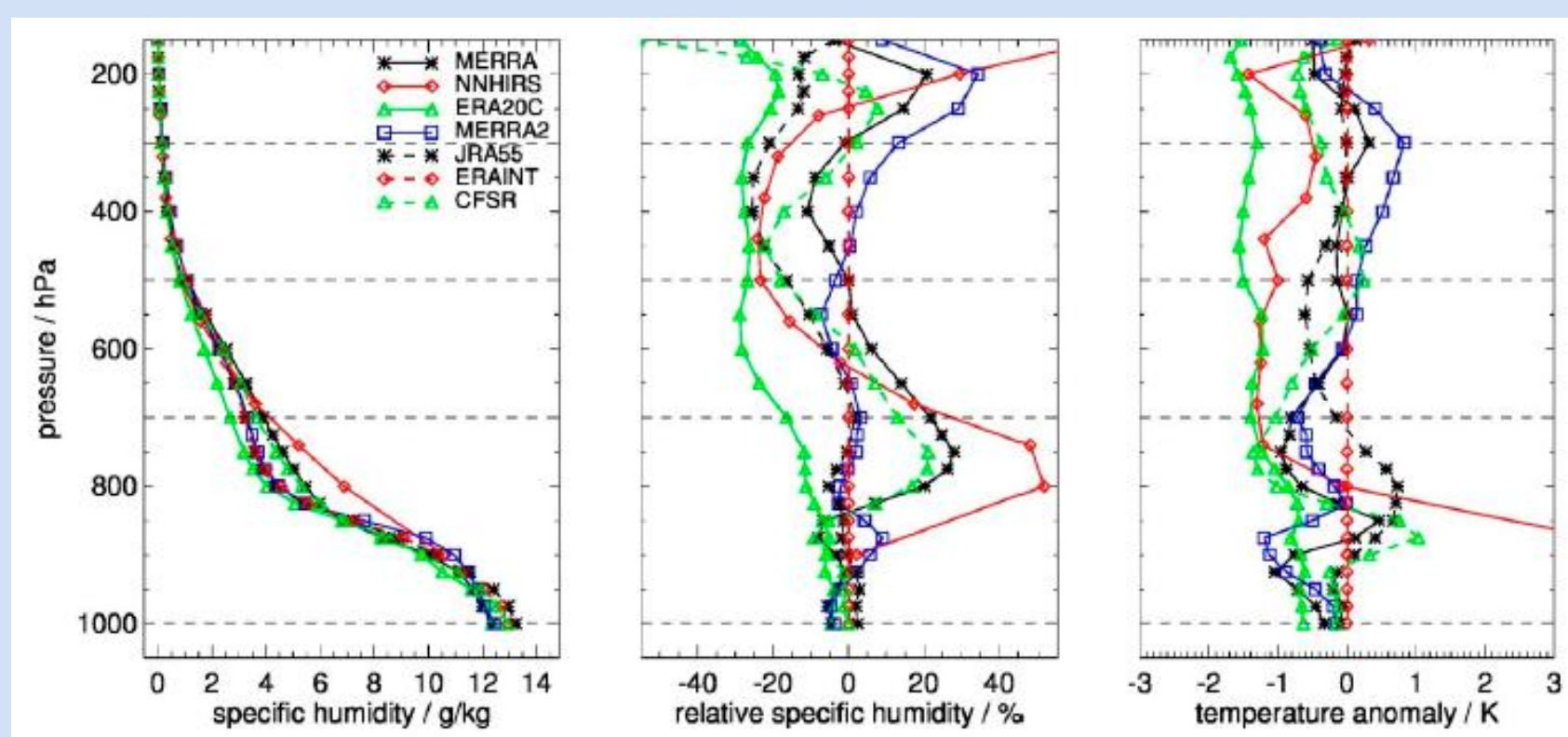


▲ Figure 2: Anomaly time series of specific humidity at 700 hPa averaged globally within 60°N/S and over Sc Pacific region (see Fig. 3). Time series were shifted by climatological averages. Vertical bars show break points using the style of the anomalies. Bars are printed in bold when PMF test (Wang, 2008a,b) and SNH test (Hawkins, 1977, Alexandersson, 1986) agree on detection time.

Date YYYY-mm	Break Size PMF	Break Size SNH	Break Size K	Data Record	Event
1988-10	-0.76			nnHIRS	NOAA11 declared operational on 1988-11-08 NOAA12 declared operational on 1991-09-17, approximate end of assimilation of NOAA10 data [23]
1991-08	0.53	0.08*		JRA-55	Start of assimilation of F11 data in 1991-12-05, end of assimilation of F08 data in 1991-12-04 and of NOAA10 MSU and HIRS data on 1991-09-17 [24]
1991-12	0.26	0.15		MERRA-2	Approximate start of assimilation of NOAA15 data (Table A1 and Figure 4 of [23], approximate end of assimilation of NOAA12 (MSU), see Figure 1 at http://www.remss.com/missions/amsu
1992-03	0.21	-0.63	-0.25	CFR	Approximate start of assimilation of NOAA15 data (Table A1 and Figure 4 of [23], approximate end of assimilation of NOAA12 (MSU), see Figure 1 at http://www.remss.com/missions/amsu
1996-06	0.41	0.13		JRA-55	Approximate end of assimilation of NOAA15 data, change from assimilation of GOESW to GOES10 data [25]
1998-10		0.85	0.52	CFR	Approximate start of assimilation of NOAA15 data, change from assimilation of GOESW to GOES10 data [25]
2001-03	-0.55	-0.73	0.89	MERRA	Start assimilation of NOAA16 on 2001-03-02 [24]
2001-04	-0.67	-0.22		CFR	Approximate start of assimilation of NOAA16 data [20]
2003-08	-0.50	-0.16*		ERA-20C	See text

▲ Table 1: Date and strength of break points and coincident changes in the observing system or changes of input to the assimilation scheme. Data basis: specific humidity at 700 hPa over Sc region (see Figs. 2 and 3), with ERA-Interim as reference. Break point size is printed in bold if PMF test and SNH test results agree on detection time. Table 1, Fig. 2 from Schröder et al. (2019)

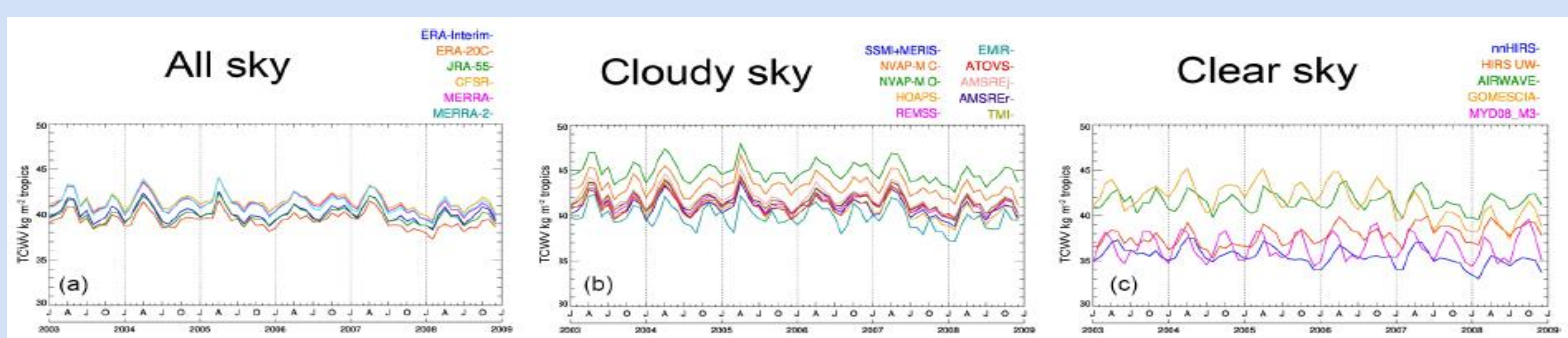
Profile inter-comparison



▲ Figure 6: Intercomparison of average specific humidity (left), relative specific humidity (middle, relative to ERA-Interim) and average temperature (right) over the Pacific stratocumulus region (see box in Figure 3) and southern hemispheric summer months. Dashed horizontal lines mark 1000, 700, 500, and 300 hPa (Schröder et al., 2019).

Inter-comparison of full archive

▼ Figure 7: Time series (January 2003–December 2008) of TCWV for the tropics (±20° N/S) over ocean for the predominant retrieval condition classes all-sky, cloudy-sky and clear-sky. Partly the legends include unambiguous abbreviations of the data record names, with the following exceptions: AMSR-E JAXA (AMSREJ), AMSR-E REMSS (AMSRE), and Merged Microwave REMSS (REMSS) (Schröder et al., 2018).

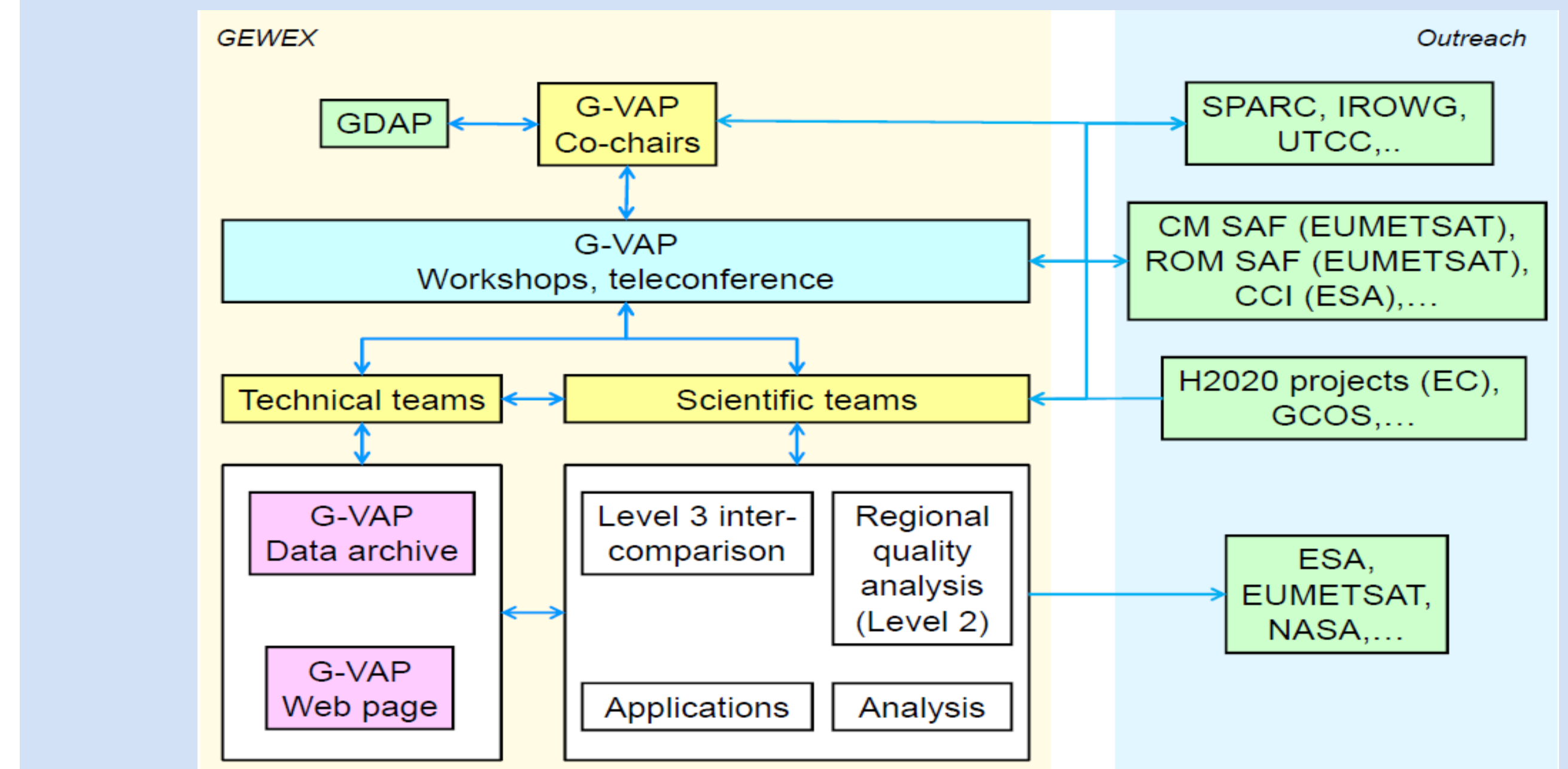


References

Alexandersson (1986, JClimate), Dessler+Davis (2010, JGR), Hawkins (1977, JASA), Mears et al. (2007, GRL), Mieruch et al. (2014, JGR), Schröder et al. (2018, ESSD, 2019, Rem Sens), Wang (2008a,b, JAOT, JAMC), Weatherhead et al. (1998, JGR)

@Climate_SAF
https://twitter.com/climate_saf

Overview

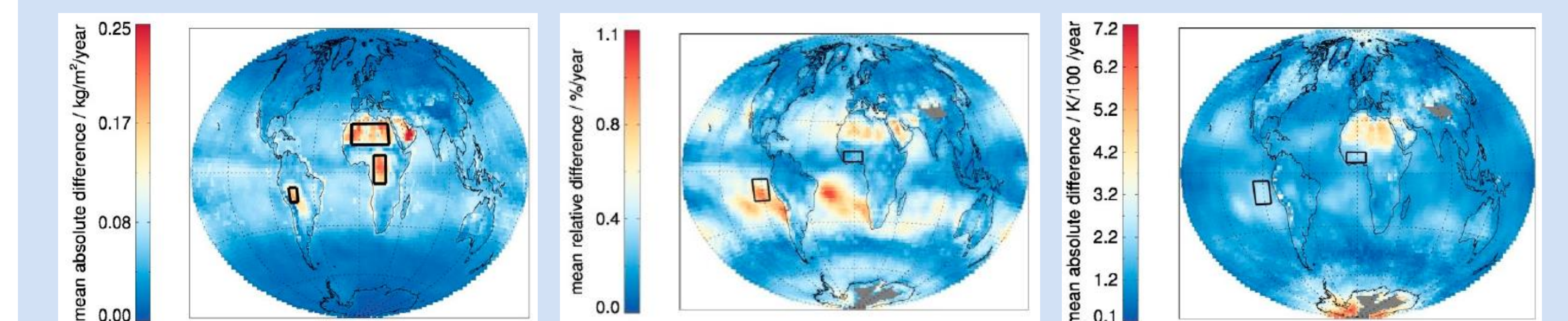


▲ Figure 1: Graphical overview of G-VAP

Data archive

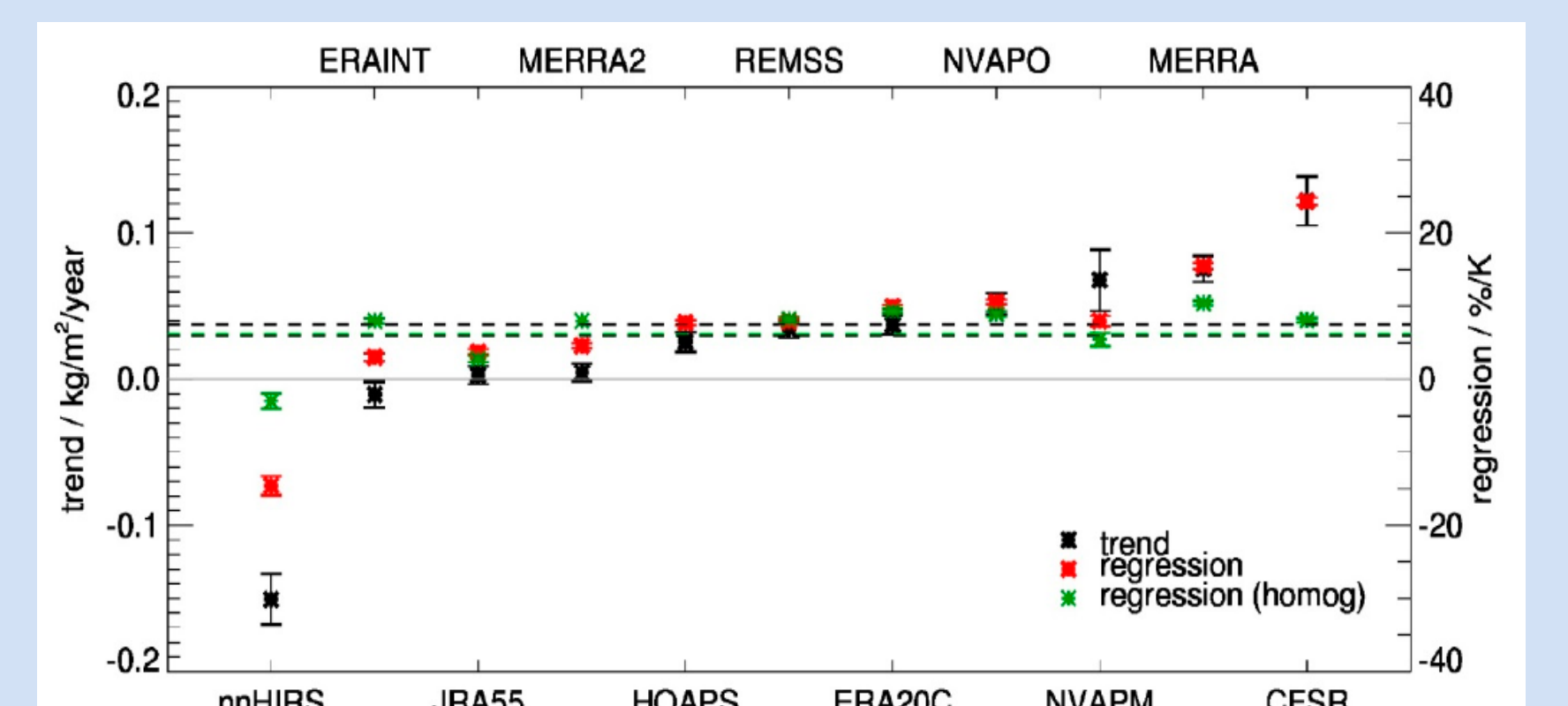
- Regridded to common grid (2°x2°, regular), common vertical levels: 1000, 700, 500, 300 hPa, common period depending on parameter (e.g., 1988-2008 for TCWV),
- Freely available via doi-reference (10.5676/EUM_SAF_CM/GVAP/V001),
- Results from intercomparison of full archive in Schröder et al. (2019), ESSD, 10.5194/essd-10-1093-2018 .

Trend estimation and regression



▲ Figure 3: Mean absolute/relative difference in trend estimates (after Weatherhead et al., 1998, Mieruch et al., 2014) for TCWV (left), specific humidity at 700 hPa (middle, here in relative units) and temperature at 700 hPa (right) (from Schröder et al. 2019).

► Figure 4: Trend estimates over global ice-free ocean (<60° N/S), sorted in ascending order and results from regression analysis (Dessler and Davis, 2010, Mears et al., 2007). Bars give 1-sigma uncertainty estimate from trend estimation. Black dashed lines mark general theoretical expectation range. Also shown are regressions after homogenisation using output from homogeneity testing (Schröder et al., 2019).



Conclusions

G-VAP provides a decent overview of available water vapour data records at <http://gewex-vap.org>. Data records with a temporal coverage of more than 10 years have been utilised in G-VAP related analysis. The regridded data records comprise the G-VAP data archive which is freely available. Differences in linear trends reveal distinct areas at central South America, central Africa, the Sahara, the Arabian Peninsula, the poles and the stratocumulus regions. In the latter case the profile data records exhibit maximum spread at and above cloud top. An analysis of anomaly differences showed that the majority of data records are affected by break points and that regions of distinct trends usually exhibit break points. Most of the break points can be attributed to changes in the observing system. The break points are a function of data record, region and parameter. Also, the trend estimates are typically significantly different and are not in line with theoretical expectation. Exceptions are HOAPS and REMSS. Finally, the spread in averaged TCWV data records as a function of predominant retrieval condition is largest in the clear-sky case. The next G-VAP workshop will take place at DMI, Copenhagen, Denmark on two days in 5-9 October 2020.

Recommendations (subset):

- CGMS, WMO, GRUAN: Aim at the sustained generation and development of a stable, bias corrected multi-station radiosonde archive including reprocessing of historical data.
- Space Agencies, PIs, G-VAP: Enhance quality analysis of profile data records over open ocean, in particular over high pressure areas/subsidence areas and stratus.
- GEWEX, Space agencies, G-VAP: It is needed to assess options to merge the various observing systems to provide long-term, high resolution water vapour profile data.
- Space Agencies: Need for inter-calibrated radiance/brightness temperature data records and homogeneously reprocessed (instantaneous) satellite data records.
- CGMS, Space agencies: It is important to ensure that developments around 5G telecommunication links do not impact microwave observations around 23 GHz via radio-frequency interference.

